Calculation of mismeasurement due to incorrect installation of orifice plate using computational fluid dynamics

National Engineering Laboratory

Add value.
Inspire trust.

Report Produced for Cadent Gas Limited

Date: August 2021

Report No: 2021_423
Project No: CGL002

Executive Summary

TÜV SÜD National Engineering Laboratory (hereinafter NEL) were contracted by Cadent Gas Limited (hereinafter Cadent) to calculate the mismeasurement of natural gas flow due to an incorrectly installed (reversed) orifice plate at the Alrewas facility operated by Cadent.

NEL used Computational Fluid Dynamics (CFD) to model two orifice plates, namely orifice plate 295-5 and orifice plate 5036, in a correct and a reversed installation for three different flow rates resulting in a total of 12 simulations.

It was found that in both instances the meter under read across the full range of Reynolds numbers modelled.

Orifice plate 295-5 had a maximum shift in discharge coefficient of 7.37 % at the maximum flowrate and plate 5036 had a maximum shift of 5.64 %.

In both cases the shift in discharge coefficient was not linear across the range of Reynolds numbers modelled, but plate 5036 had only a minor deviation from linearity.

In addition to these simulations further work was undertaken to model experimental work carried out at SwRI to determine how well CFD predicted the shift in discharge coefficients. In both cases analysed the shift in discharge coefficient predicted by CFD was within 1 % of the shift obtained from the experimental work.

The results from plate 295-5 are shown in the table below:

Case (Reynolds number)	Discharge Coefficient - CFD Ideal	Discharge Coefficient - CFD Reversed	Shift In Discharge Coefficient (%)
Low Flow (Re 7,095,465)	0.59706	0.63556	6.45
Medium Flow (Re 14,190,929)	0.59377	0.63465	6.88
Maximum Flow (Re 26,607,993)	0.59119	0.63475	7.37

The results from plate 5036 are shown in the table below:

Case (Reynolds number)	Discharge Coefficient - CFD Ideal	Discharge Coefficient - CFD Reversed	Shift In Discharge Coefficient (%)
Low Flow (Re 7,095,465	0.59496	0.62663	5.32
Medium Flow (Re 14,190,929)	0.59386	0.62559	5.34
Maximum Flow (Re 26,607,993)	0.59133	0.62469	5.64

Table of Contents

1. INTRODUCTION

NEL were contracted by Cadent to calculate the mismeasurement of natural gas due to an incorrectly installed (reversed) orifice plate. After consideration of the project brief it was decided that Computational Fluid Dynamics (CFD) was the most suitable approach.

ISO 5167 Part 2 outlines the correct procedure for installing an orifice plate as part of a fiscal metering system. The work carried out in this report compares the discharge coefficient calculated from a CFD analysis for an orifice plate installed as per ISO 5167 Part 2 against the calculated discharge coefficient for the orifice plate when it has been installed in the reversed orientation.

This process is carried out over a range of different Reynolds numbers to determine the effect of Reynolds number on the shift in discharge coefficient, and thus the measurement error. Often when an orifice plate is installed incorrectly the shift in discharge coefficient is not linear across a range of Reynolds numbers.

2. SCOPE OF WORK

As per quotation NEL-16952 V-05 [2] the following scope was undertaken:

- A high resolution scan of orifice plates, 295-5 and 5036
- CFD analysis was undertaken to compare an ideal installation to the reversed orientation for each orifice plate at 3 flowrates
- The flow measurement error was calculated using data from the CFD analysis.

The modelled flowrates are shown below in Table 1.

TABLE 1: SIMULATED CASES

Case	Inlet Velocity (ms^{-1})	Density (kgm^{-3})	Viscosity ($kgm^{-1}s^{-1}$)	Reynolds Number	Mass Flowrate (kgs^{-1})
Low	4	49.38	1.20×10^{-5}	7,095,190	28.98
Medium	8	49.38	1.20×10^{-5}	14,190,381	57.96
High	15	49.38	1.20×10^{-5}	26,606,964	108.67

3. SIMULATED CASES

The flow measurement error resulting from the incorrect installation of the orifice plate is a function of Reynolds number and therefore it is important to undertake simulations which cover the operating envelope of the system.

In order to do this NEL modelled 3 different flowrates (for each orifice plate), namely low, medium, and high flow rates, as shown in Table 1. The flowrates modelled were chosen by Dr Michael Reader-Harris who is acting as

the Independent Technical Expert in this case. A total of 12 cases were studied: 3 for each ideal installation (standard orifice plate) and 3 for each reversed orifice plate.

4 CFD MODEL

The commercial CFD software package, ANSYS FLUENT 2021 R1 was used for all simulations. An overview of the geometry, mesh and models used is given in section 4.1 to 4.5.

4.1 Ideal Geometry

In order to capture the as found condition of the orifice plates, a high accuracy laser scan was undertaken by Physical Digital [2]. In order to produce the 3D CAD model of the orifice plates it was necessary to reverse engineer the Standard Tessellation Language (STL) file which is produced from the laser scan to create a closed geometry. The deviation between the STL surface and the reversed engineered CAD is shown below in Figure 1 and Figure 2.

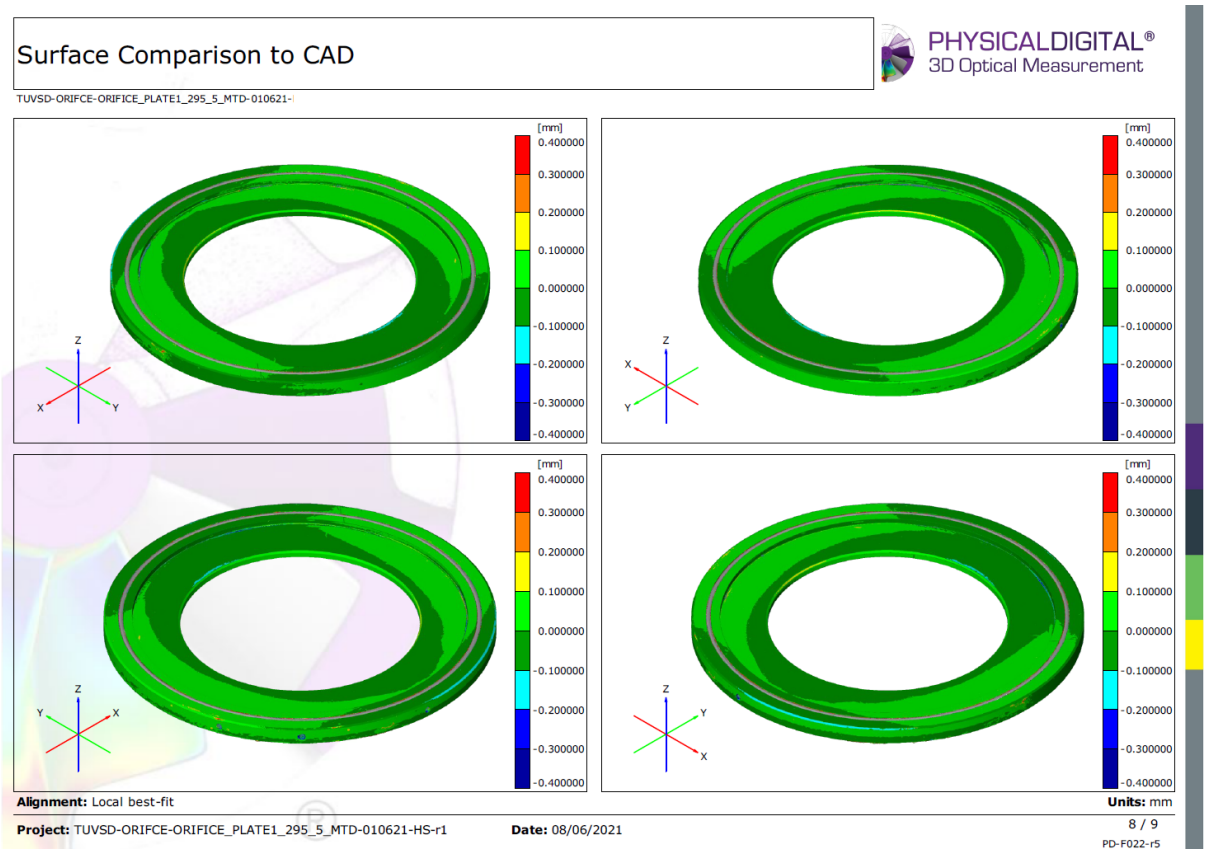

FIGURE 1: SURFACE COMPARISON TO CAD VIEW 1 – PLATE 295-5

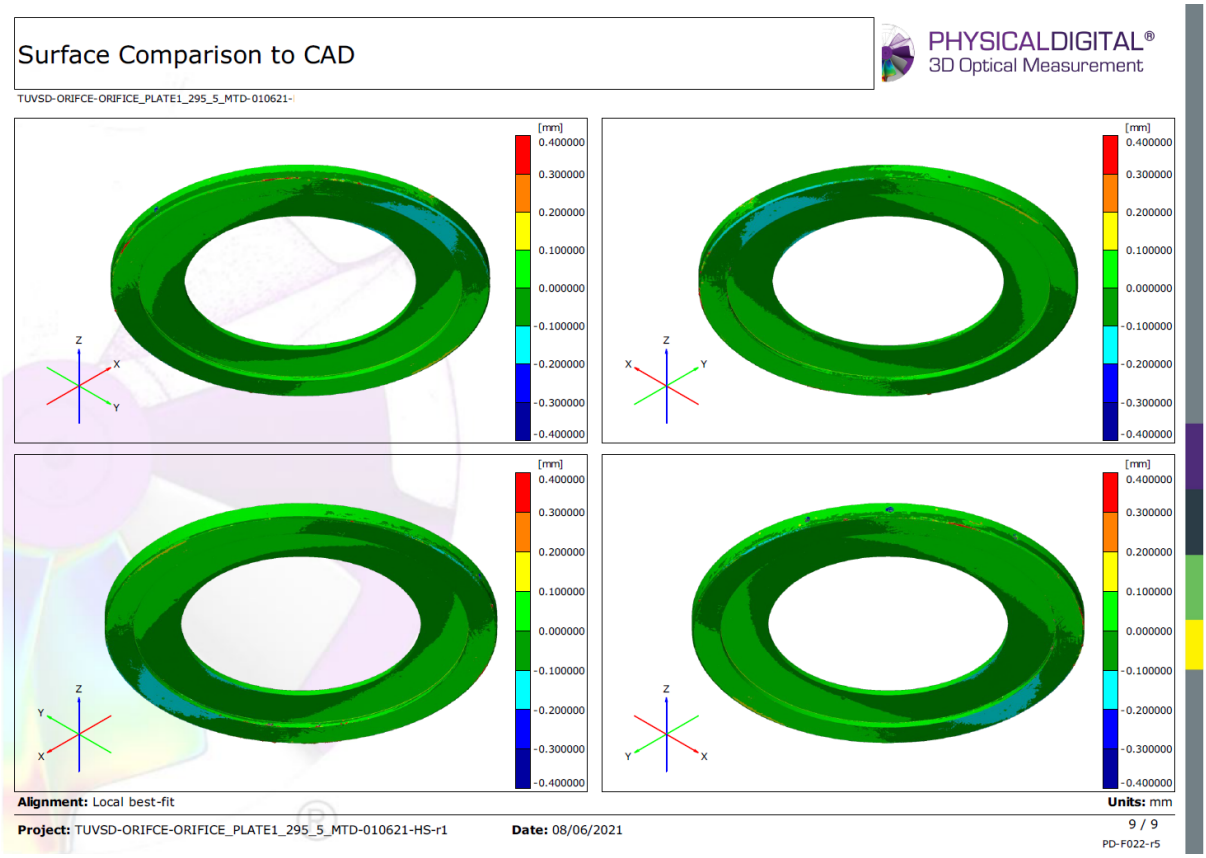

FIGURE 2: SURFACE COMPARISON TO CAD VIEW 1 – PLATE 295-5

4.1.1 Plate ALREWAS-295-5

The reverse engineered model of the Orifice Plate obtained from the laser scan is shown in Figure 1. Figure 2 shows a section view through the 3D CAD representation of the Orifice Plate. The sharp edge and bevel are shown in detail in Figure 3.

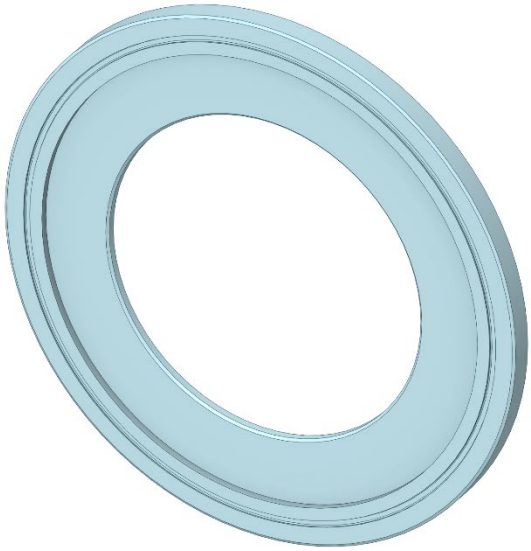

FIGURE 3: ISOMETRIC VIEW OF ORIFICE PLATE – PLATE 295-5

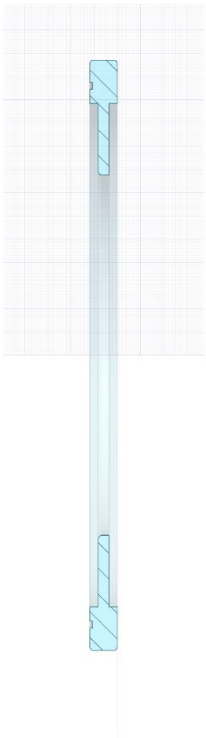

FIGURE 4: SECTION VIEW OF ORIFICE PLATE – PLATE 295-5

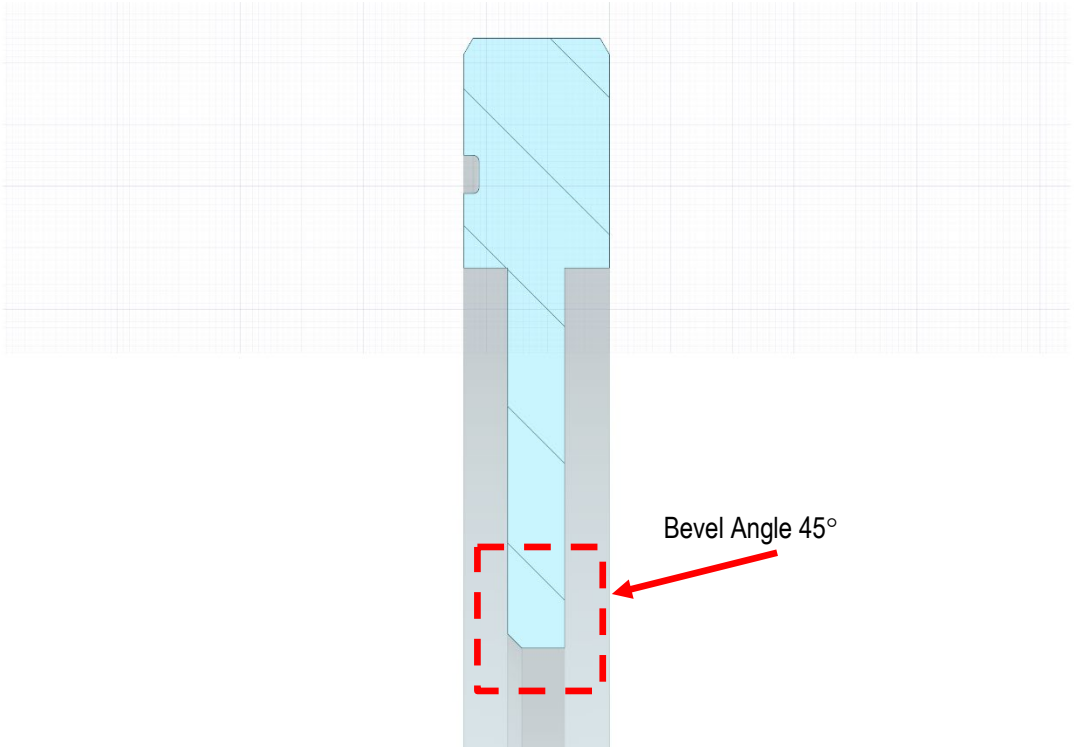

FIGURE 5: SECTION VIEW OF ORIFICE PLATE SHOWING BEVEL IN DETAIL – PLATE - 295-5

In order to reduce the computational time symmetry was exploited and a quarter symmetry model was used. This was only possible as at the time of undertaking this analysis the drawings of the piping configuration were not available and these were measured by hand externally on site. As the internal dimensions of the pressure tappings were not available these were omitted from the model, thus the geometry and flow are symmetrical.

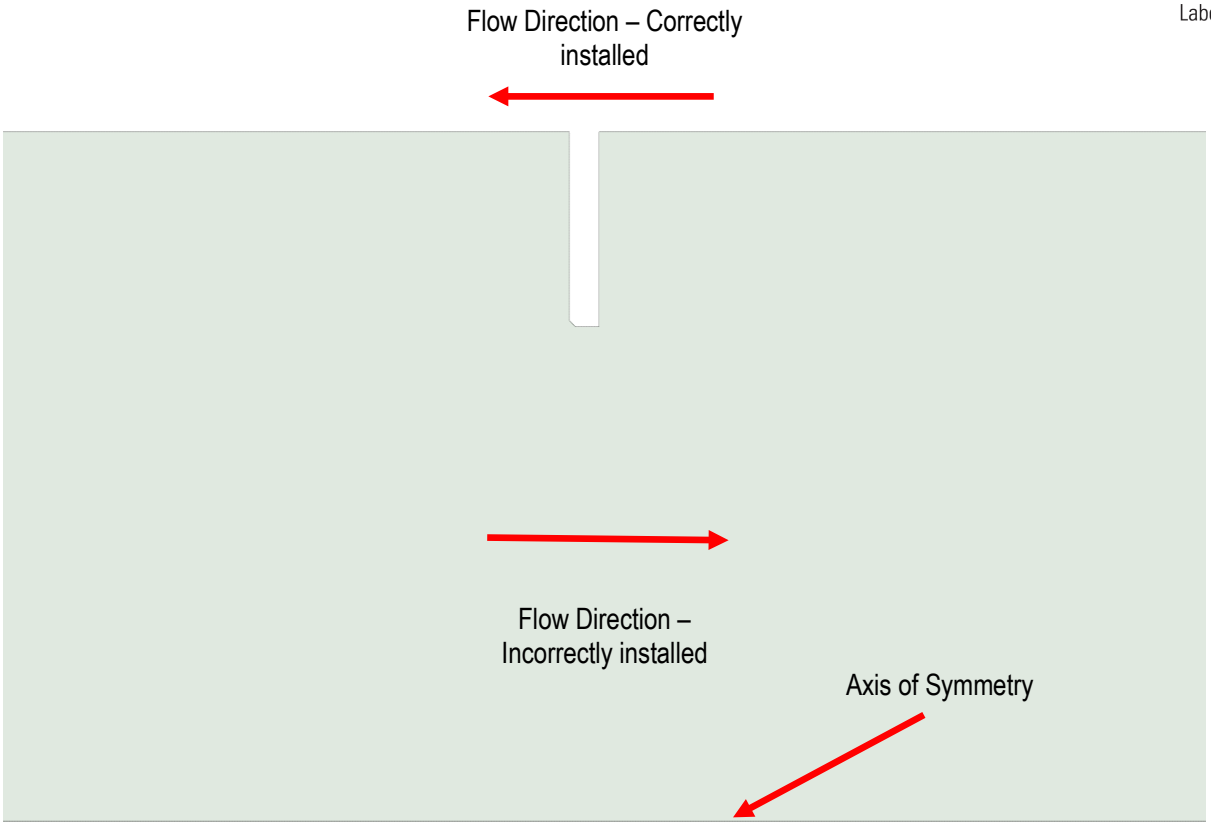

FIGURE 6: QUARTER SYMMETRY MODEL – PLATE 295-5

4.1.2 Plate ALREWAS-5036

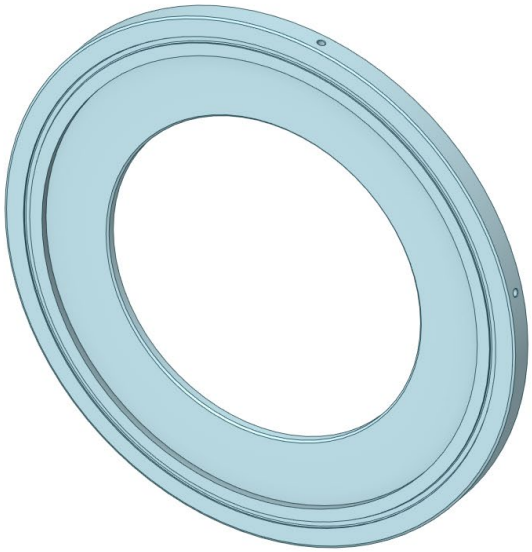

FIGURE 7: ISOMETRIC VIEW OF ORIFICE PLATE – PLATE 5036

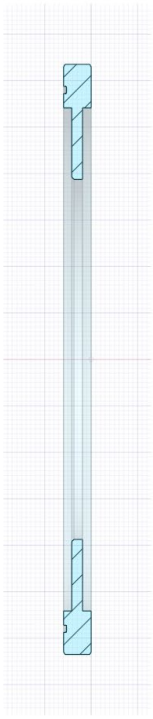

FIGURE 8: SECTION VIEW OF ORIFICE PLATE – PLATE 5036

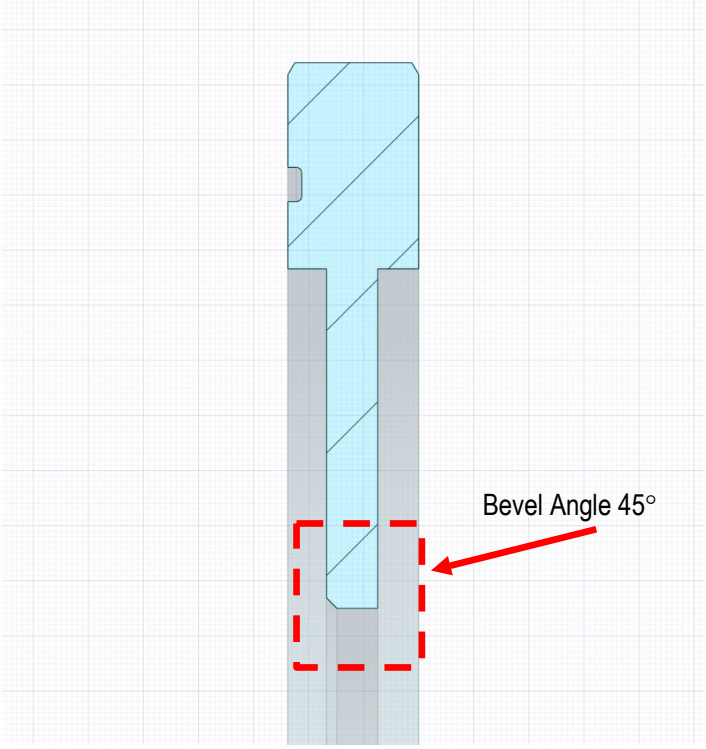

FIGURE 9: SECTION VIEW OF ORIFICE PLATE SHOWING BEVEL IN DETAIL – PLATE - 5036

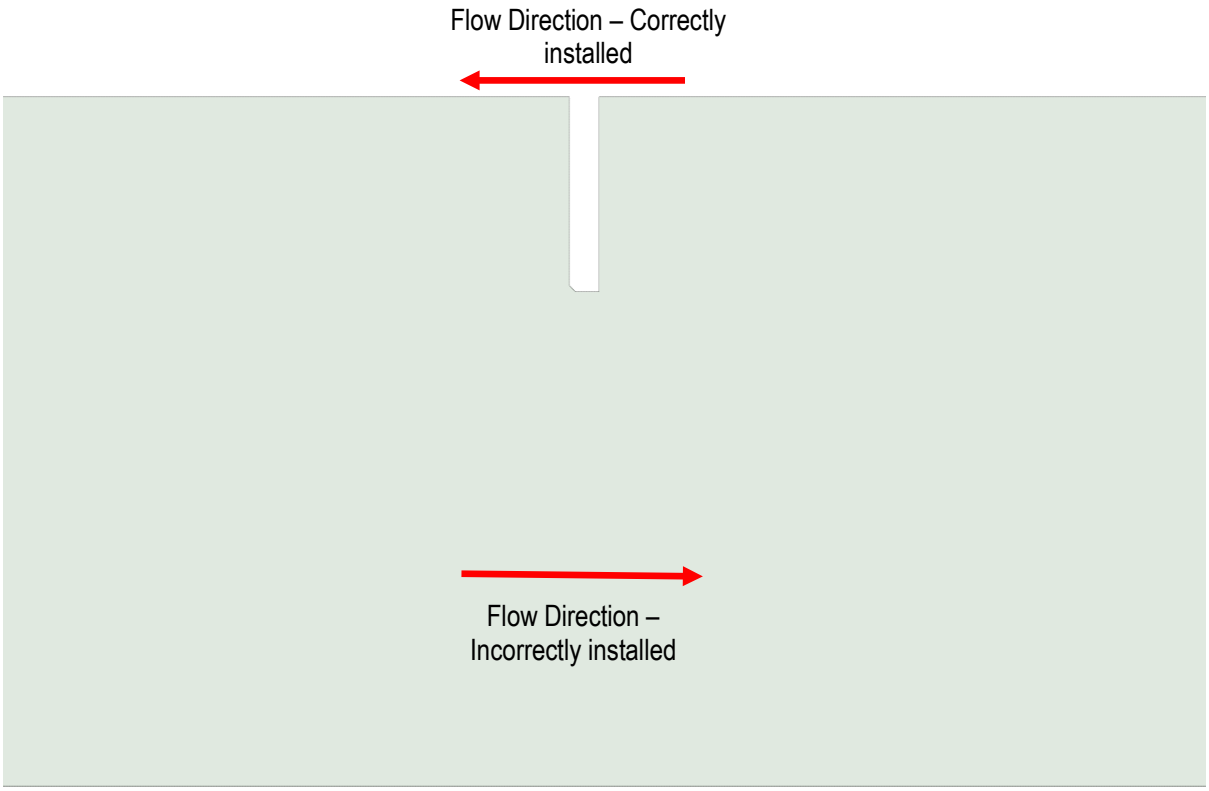

FIGURE 10: QUARTER SYMMETRY MODEL – PLATE 5036

4.2 Mesh

The partial differential equations that govern fluid mechanics are highly non-linear and must be solved numerically. Therefore, the flow domain is split into smaller sub domains (i.e. cells). The governing equations are then numerically discretised and solved inside each of these subdomains. The subdomains are often referred to as finite volumes, elements or cells, and the collection of all elements is called a mesh.

4.2.1 Overview of Meshing Approach

In this case a very high quality unstructured polyhedral mesh, with local refinement (i.e. smaller cell size) around the sharp edge of the orifice plate was used for the ideal cases. The surface mesh is shown in Figures 11 to 13. A high level of refinement has been used in the vicinity of the orifice plate. This is critical because the pressure drop measured is driven primarily by separation which occurs at the sharp edge.

A refined boundary layer mesh has been applied throughout the model to ensure that the values of y+ throughout the domain are appropriate for the use of wall functions.

An example of the volume mesh in the vicinity of the orifice plate is shown in Figure 14.

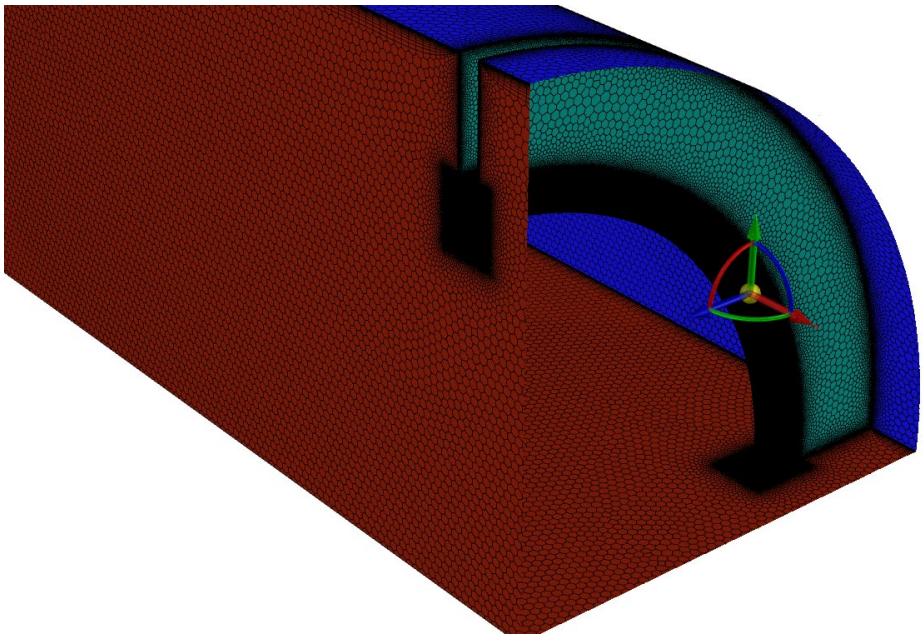

FIGURE 11: SURFACE MESH SHOWING HIGH DEGREE OF REFINEMENT ON SHARP EDGE

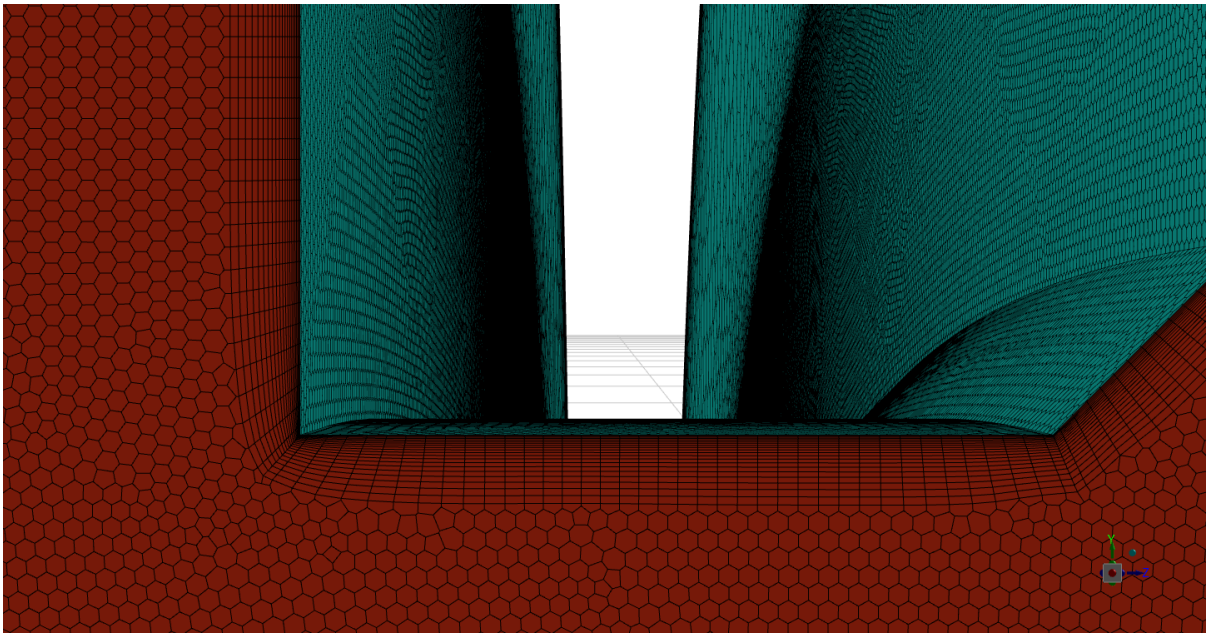

FIGURE 12: SURFACE MESH SHOWING REFINED BOUNDARY LAYER MESH ON ORIFICE PLATE

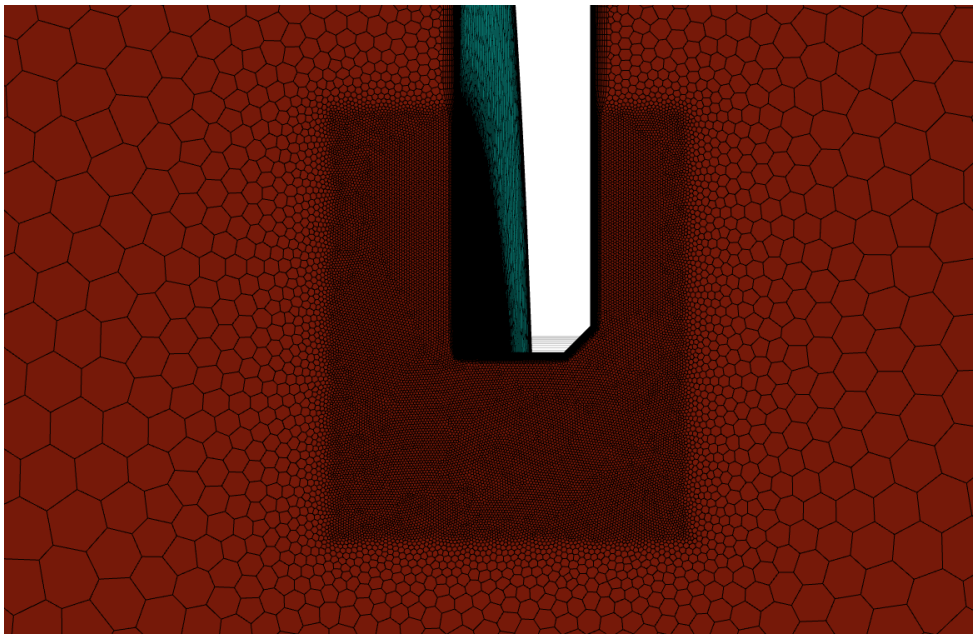

FIGURE 13: SURFACE MESH SHOWING REFINEMENT IN VICINITY OF THE ORIFICE PLATE

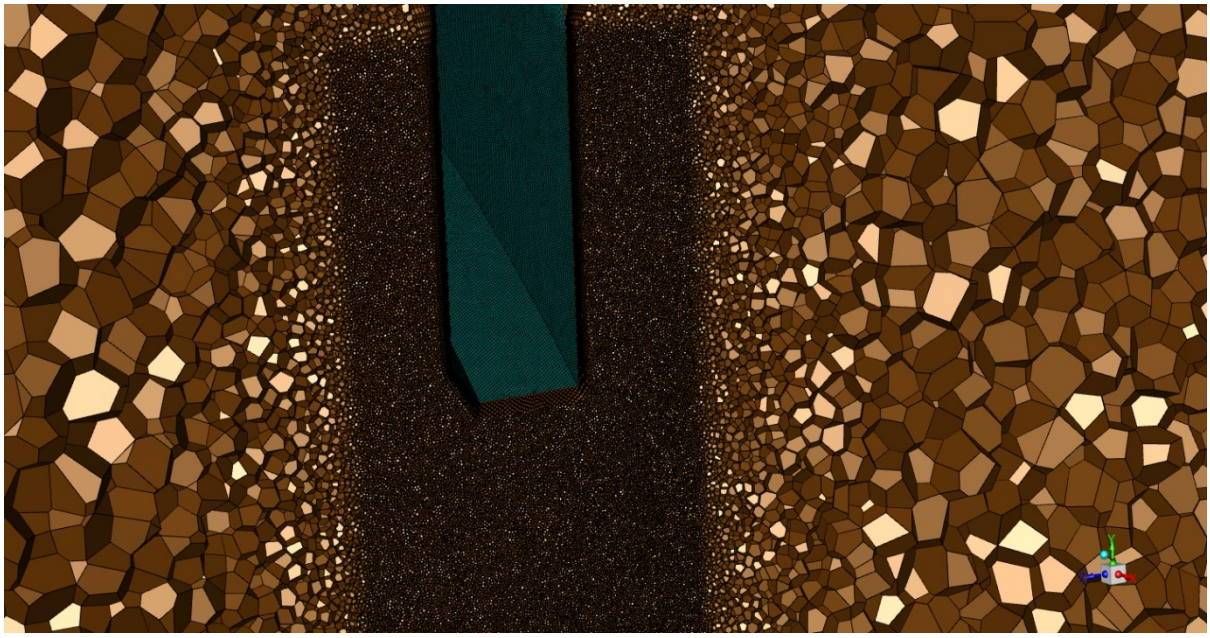

FIGURE 14: VOLUME MESH IN VICINITY OF ORIFICE PLATE

4.3 Mesh Independence

In any CFD simulation it is important to ensure that the solution is mesh independent, (i.e. the solution is not dependent on the mesh density and further refinement does not change the output of the simulation). In this case given the similarity of the physics, a mesh independence study was performed on only one plate. Simulations were performed for plate 5036 with the orifice plate installed in the correct orientation.

During the meshing process a body of influence (BOI) approach was used to locally control the sizing of the cells in regions of the simulation. Two body of influences were used, namely BOI1 and BOI2, and these are shown below in Figure 15 and Figure 16.

BOI's can be used to apply sizes to certain regions of the mesh to capture high gradients and other flow features. In this case, BOI1 was used to ensure the sharp edge of the plate and the bevel were captured with sufficient mesh resolution; BOI2 was used to control the growth from the small cells in BOI1 such that the high velocity jet downstream of the orifice plate is captured sufficiently. This is the most effective way of capturing such effects whilst allowing the mesh to coarsen in areas far away from these high gradients.

Table 2 shows that the mesh used is grid independent. The mesh can be considered independent using the BOI 1 sizing of 0.4 mm since upon refinement the solution was changed by a maximum of 0.12 %. The uncertainty requirement for fiscal metering of gas using an orifice plate is 1 %.

Despite mesh independence being achieved using a BOI 1 sizing of 0.4 mm, the finer mesh which used a size of 0.2 mm was used for all simulations. This resulted in a mesh size of approximately 40 million cells for each model.

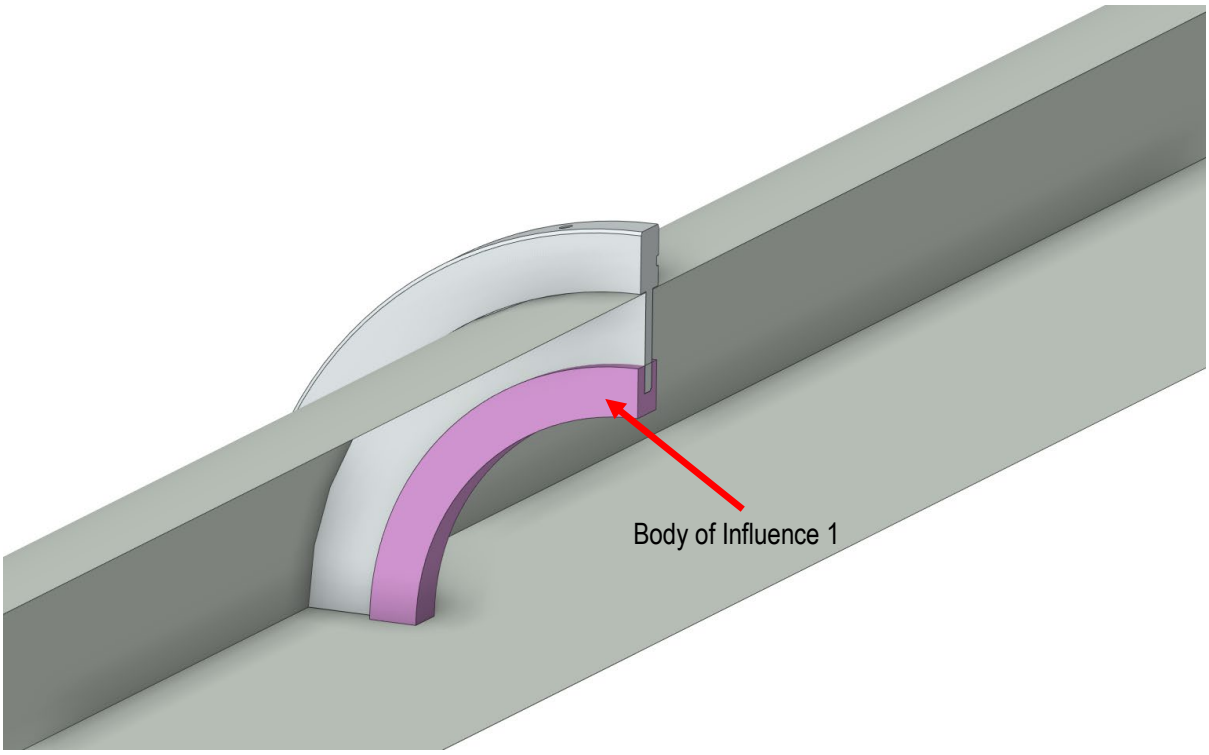

FIGURE 15: BODY OF INFLUENCE 1

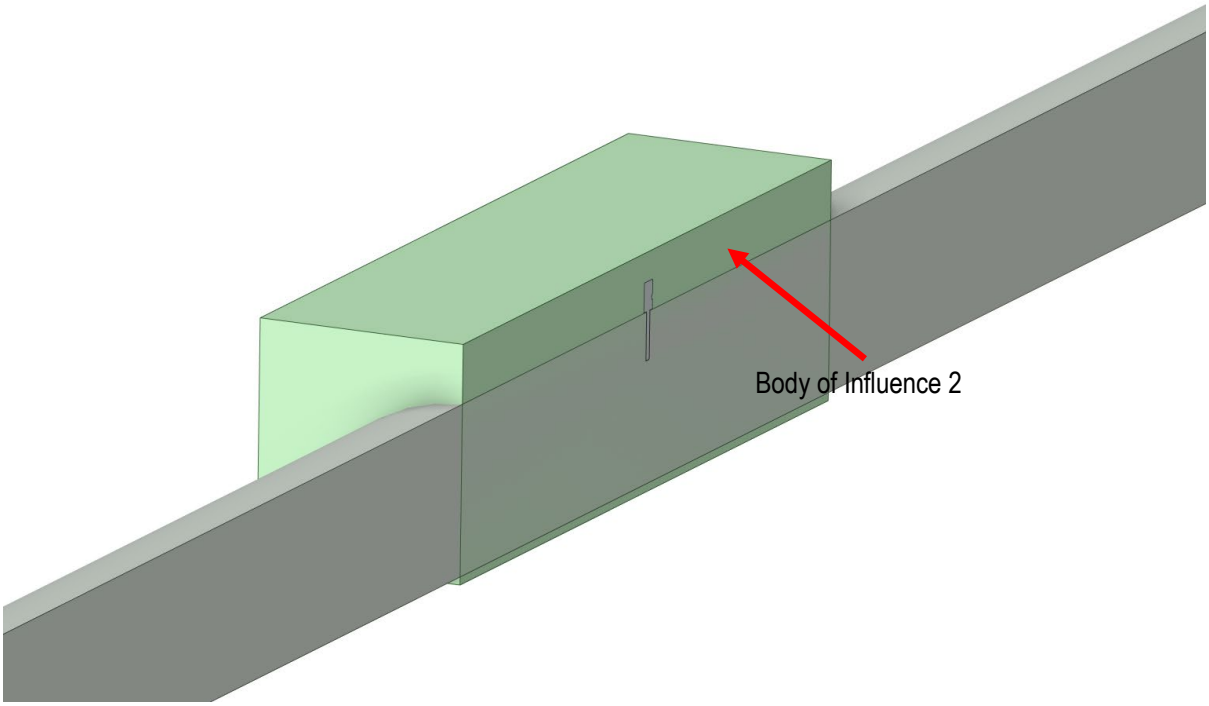

FIGURE 16 BODY OF INFLUENCE 2

TABLE 2: GRID INDEPENDENCE RESULTS

Case	BOI 1 Cell Size (mm)	BOI 2 Cell Size (mm)	Max Mesh Size (mm)	Discharge Coefficient (Ideal)	Difference (%)
Low Flow (Plate 5036)	0.2	4	12	0.59496	**0.10**
Low Flow (Plate 5036)	0.4	4	12	0.59553	
Medium Flow (Plate 5036)	0.2	4	12	0.59386	**0.11**
Medium Flow (Plate 5036)	0.4	4	12	0.59452	
Maximum Flow (Plate 5036)	0.2	4	12	0.59133	**0.12**
Maximum Flow (Plate 5036)	0.4	4	12	0.59203	

4.4 Boundary Conditions

Table 3 shows the boundary conditions that were applied to the ideal and reversed orifice plate models.

TABLE 3: BOUNDARY CONDITIONS FOR CFD MODEL

Case	Inlet Velocity (ms^{-1})	Density (kg/m^3)	Viscosity ($kgm^{-1}s^{-1}$)	Reynolds Number	Mass Flowrate (kgs^{-1})
Low	4	49.38	1.20×10^{-5}	7,095,190	28.98
Medium	8	49.38	1.20×10^{-5}	14,190,381	57.96
High	15	49.38	1.20×10^{-5}	26,606,964	108.67

4.5 Turbulence

A steady state CFD simulation was performed and a k-ϵ realisable turbulence model was used. Laminar and turbulent flows are significantly affected by the presence of walls and therefore adequate refinement is required to capture the large gradients between the bulk flow and the wall. The enhanced wall treatment function was used to model this large gradient and is applicable for a wide range of Reynolds numbers.

5. Results

All results shown in this section (for both plates) refer to the maximum flowrate case i.e. 108.67 kg/s.

5.1 Plate ALREWAS-295-5

5.1.1 Correct Installation

Contours of differential pressure for the case where orifice plate 295-5 is installed correctly are shown in Figure 17. Velocity contours are also shown in Figure 18 and Figure 19. Figure 20 shows streamlines coloured by velocity.

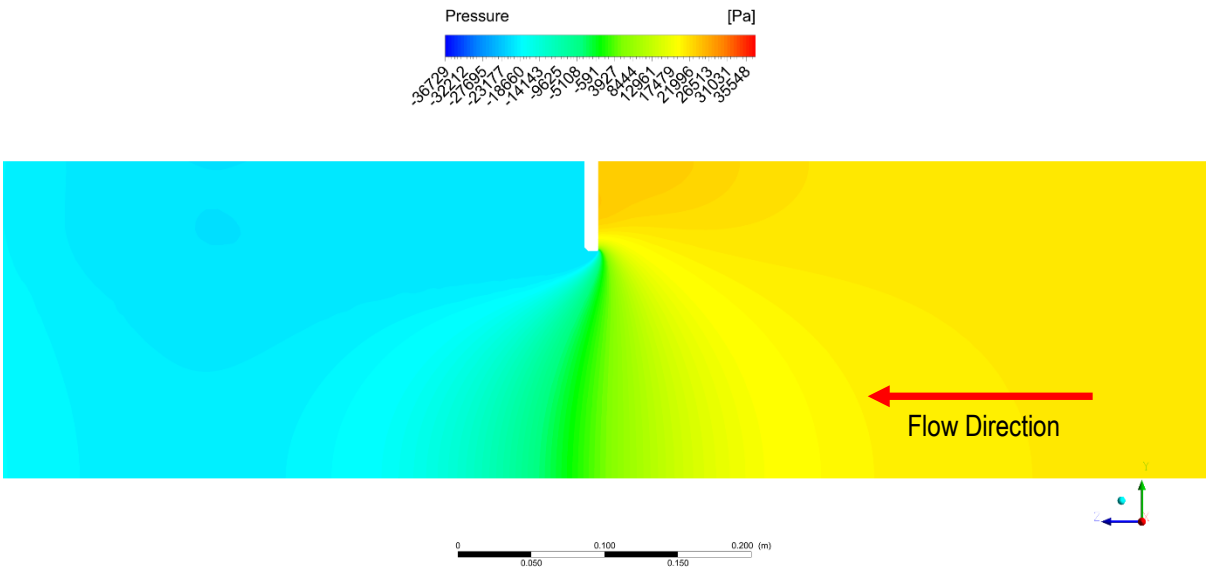

FIGURE 17: DIFFERENTIAL PRESSURE CONTOURS FOR CORRECT ORIFICE PLATE INSTALLATION SHOWING ORIFICE PLATE IN DETAIL – PLATE 295-5

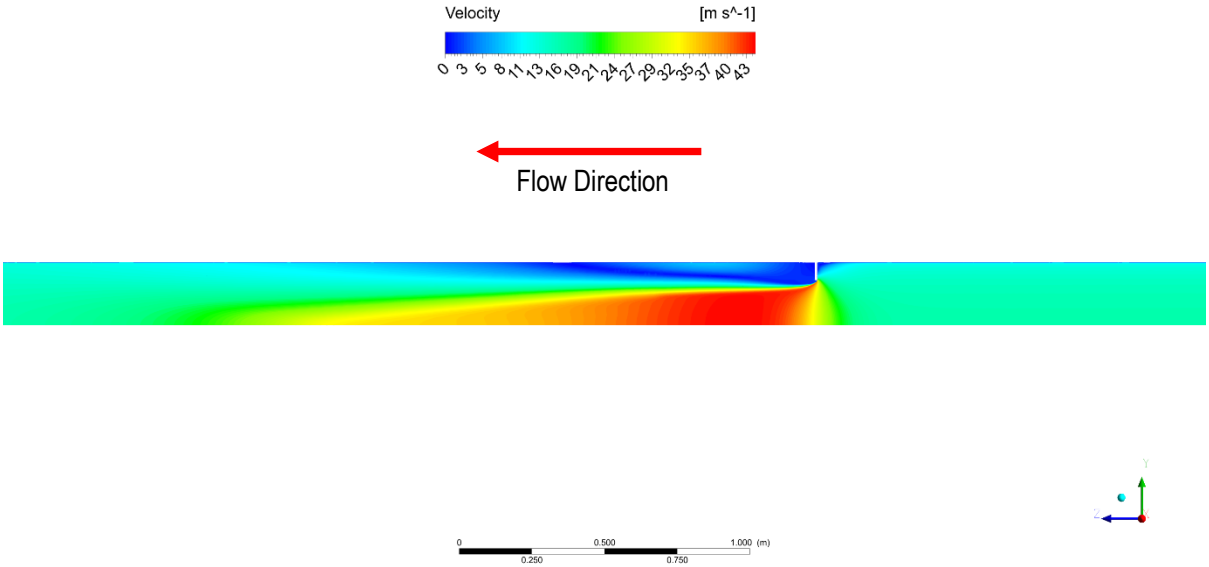

FIGURE 18: VELOCITY CONTOURS FOR CORRECT ORIFICE PLATE INSTALLATION– PLATE 295-5

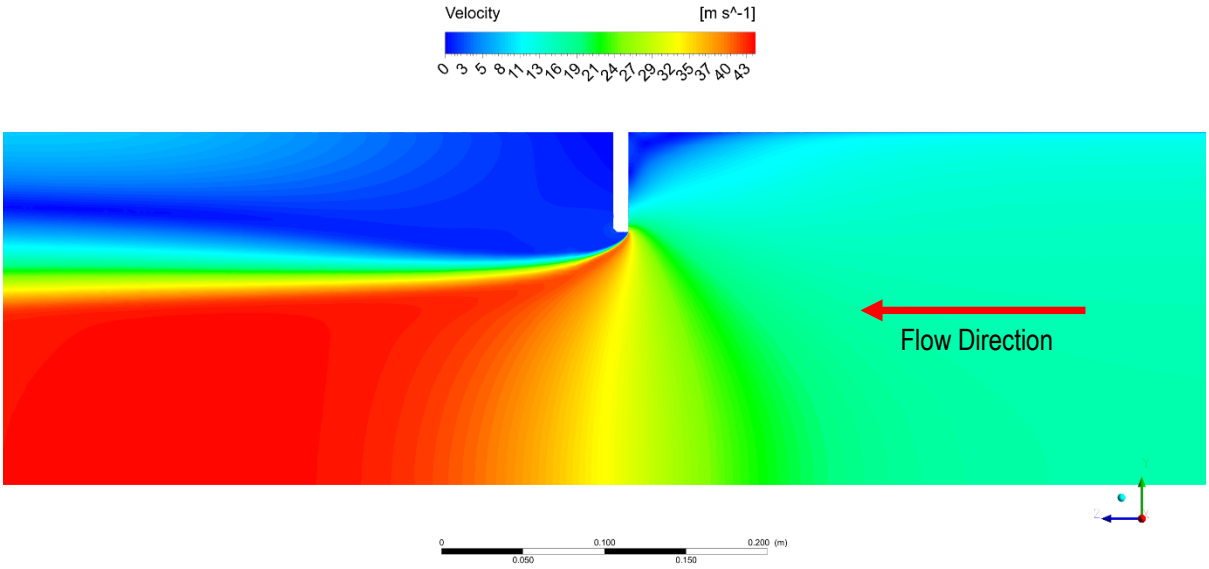

FIGURE 19: VELOCITY CONTOURS FOR CORRECT ORIFICE PLATE INSTALLATION SHOWING ORIFICE PLATE IN DETAIL – PLATE 295-5

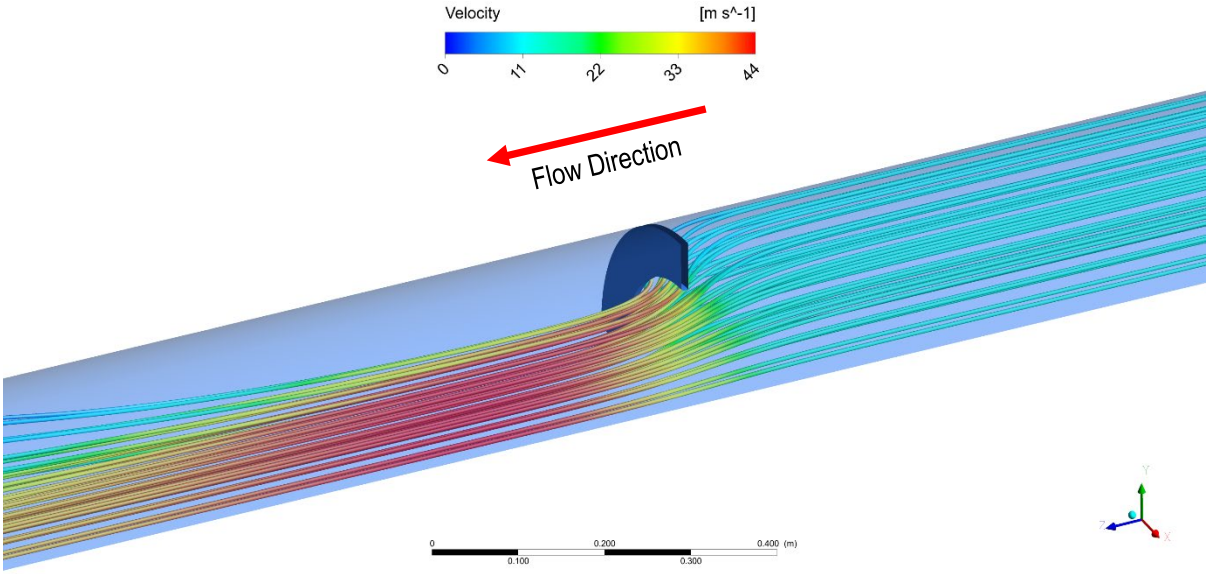

FIGURE 20: STREAMLINES COLOURED BY VELOCITY FOR CORRECT ORIFICE PLATE INSTALLATION– PLATE 295-5

5.1.2 Reverse Installation

Contours of differential pressure for the case where orifice plate 295-5 is installed in the reverse orientation are shown in Figure 21. Velocity contours are also shown in Figure 22 to Figure 24. It can be observed that when the orifice plate is installed in the reverse orientation the velocity profile is different since the separation occurs from

the bevel rather than from this sharp edge. This has a significant effect on the pressure drop and therefore contributes to a flow measurement error.

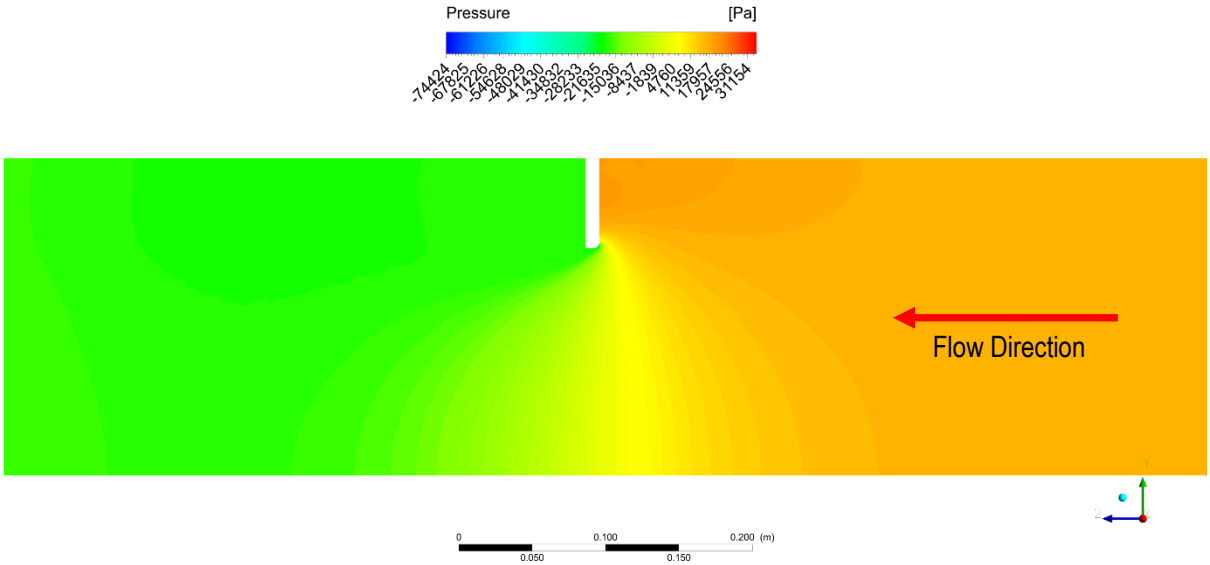

FIGURE 21: DIFFERENTIAL PRESSURE CONTOURS FOR INCORRECT ORIFICE PLATE INSTALLATION SHOWING ORIFICE PLATE IN DETAIL – PLATE 295-5

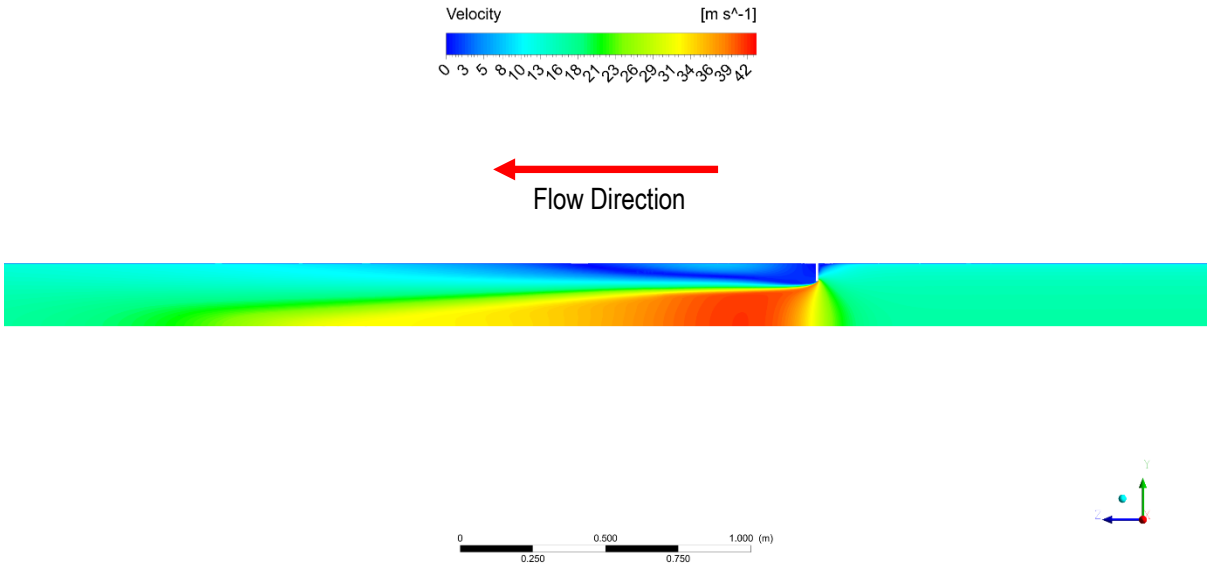

FIGURE 22: VELOCITY CONTOURS FOR INCORRECT ORIFICE PLATE INSTALLATION– PLATE 295-5

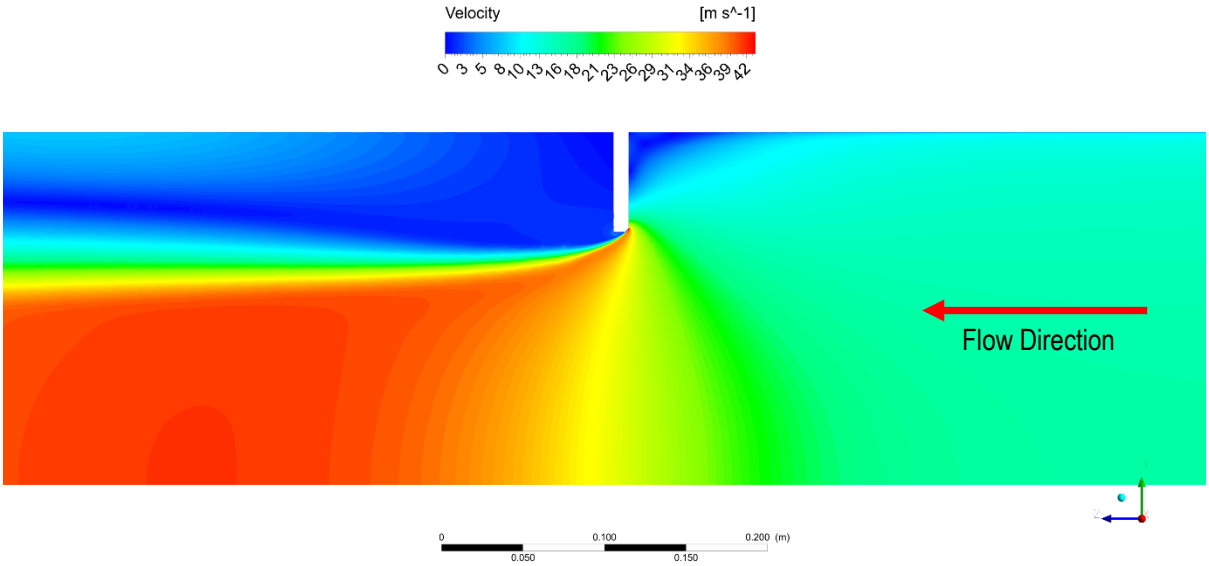

FIGURE 23: VELOCITY CONTOURS FOR INCORRECT ORIFICE PLATE INSTALLATION SHOWING ORIFICE PLATE IN DETAIL – PLATE 295-5

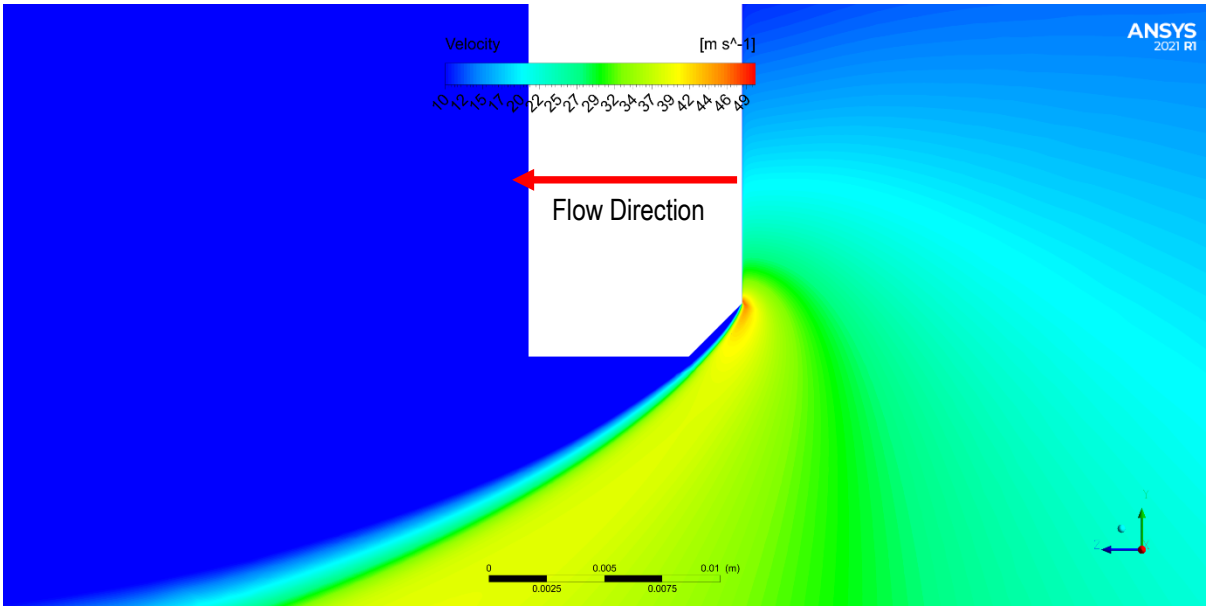

FIGURE 24: VELOCITY CONTOURS FOR INCORRECT ORIFICE PLATE INSTALLATION SHOWING SHARP EDGE & BEVEL IN DETAIL – PLATE 295-5

5.1.3 Discharge Coefficients Plate 295-5

Table 4 shows the computed discharge coefficient for plate 295-5 installed correctly and the discharge coefficient calculated from the ISO 5167 standard. All of the computed discharge coefficients are in agreement with the ISO 5167 standard and are within 1 % with the best agreement being 0.1 % at the low flow rate.

Table 5 shows the computed ideal discharge coefficient from the CFD simulation, the computed discharge coefficient for the incorrectly installed orifice plate from the CFD analysis and the corresponding shift in

discharge coefficient due to incorrect installation. It can be seen that the shift in discharge coefficient is not linear across the range of Reynolds numbers modelled and the meter is predicted to under read at all points.

TABLE 4: AGREEMENT BETWEEN CFD MODEL OF PLATE 295-5 INSTALLED CORRECTLY & ISO 5167

Case	Discharge Coefficient - Standard [1]	Discharge Coefficient - CFD Ideal	CFD Ideal Case Deviation From Standard (%)
Low Flow	0.59767	0.59706	-0.10266
Medium Flow	0.59701	0.59377	-0.54306
Maximum Flow	0.59653	0.59119	-0.89592

TABLE 5 COMPUTED DISCHARGE COEFFICIENTS & FLOW METERING ERROR FOR PLATE 295-5

Case	Discharge Coefficient - CFD Ideal	Discharge Coefficient - CFD Reversed	Shift In Discharge Coefficient (%)
Low Flow	0.59706	0.63556	6.45
Medium Flow	0.59377	0.63465	6.88
Maximum Flow	0.59119	0.63475	7.37

5.2 Plate 5036

5.2.1 Correct Installation

Contours of differential pressure for the case where orifice plate 5036 is installed correctly are shown in Figure 25 and Figure 26. Velocity contours are also shown in Figure 27 and Figure 28.

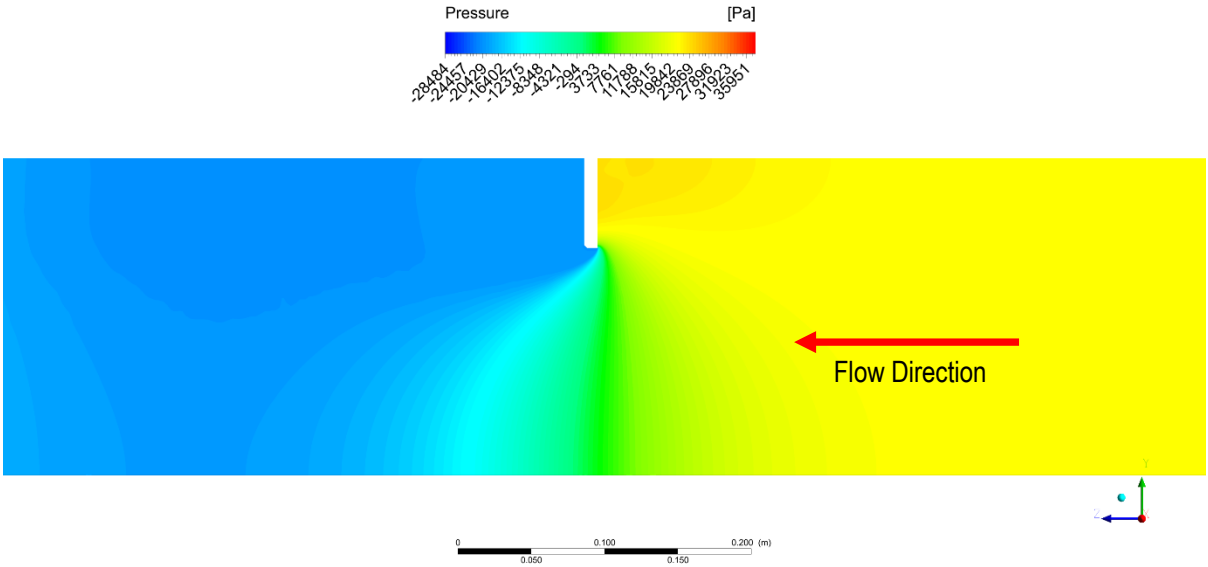

FIGURE 25: DIFFERENTIAL PRESSURE CONTOURS FOR CORRECT ORIFICE PLATE INSTALLATION – PLATE 5036

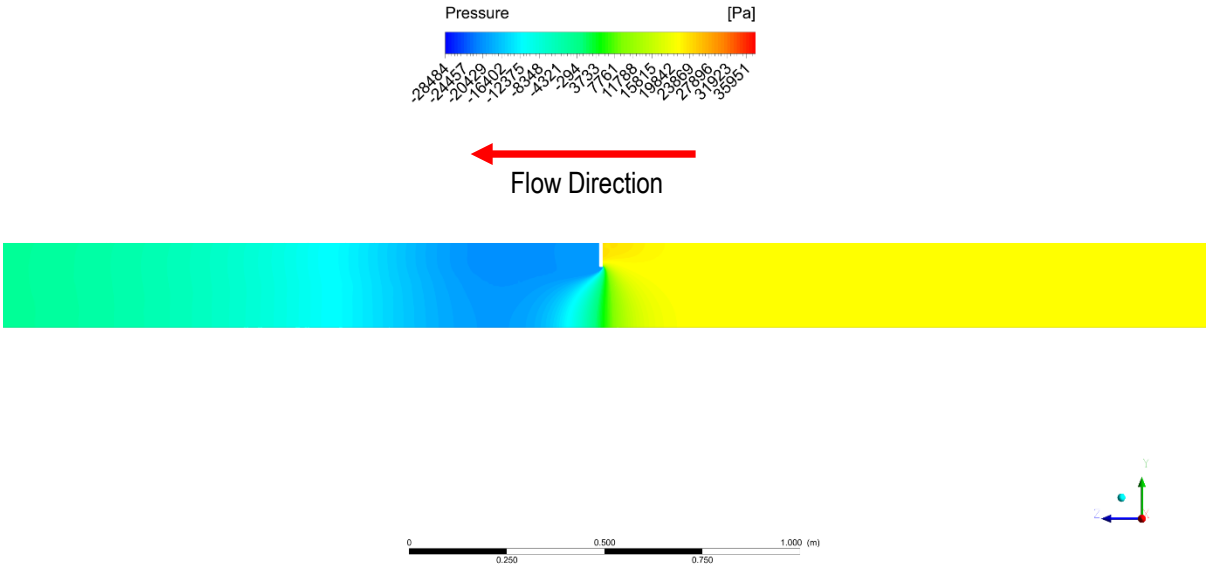

FIGURE 26: DIFFERENTIAL PRESSURE CONTOURS FOR CORRECT ORIFICE PLATE INSTALLATION SHOWING ORIFICE PLATE IN DETAIL – PLATE 295-5

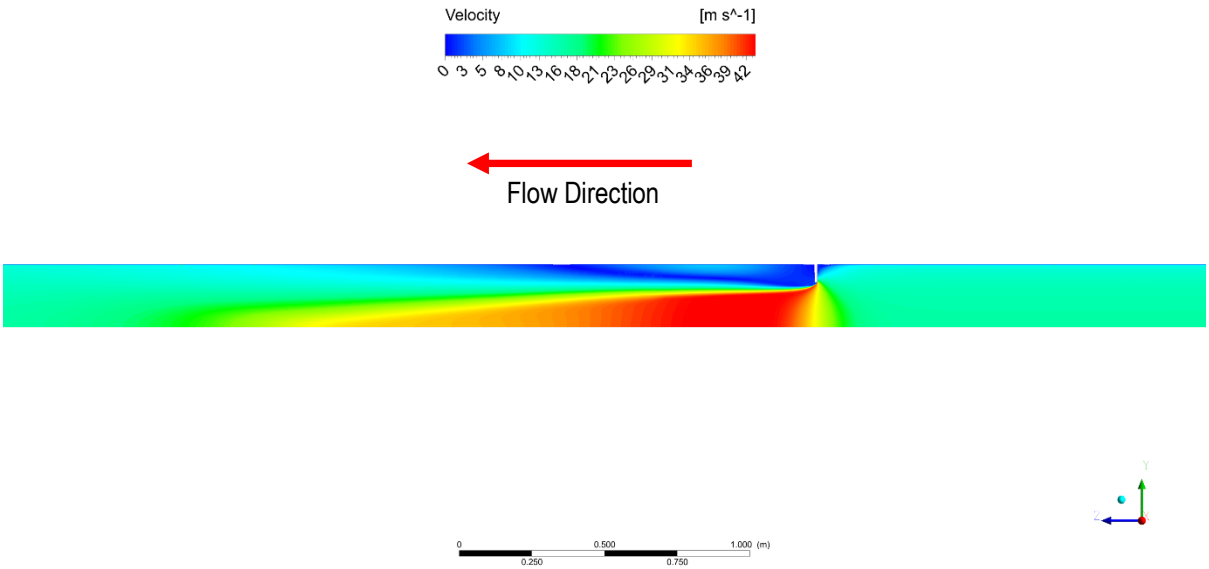

FIGURE 27: VELOCITY CONTOURS FOR CORRECT ORIFICE PLATE INSTALLATION– PLATE 5036

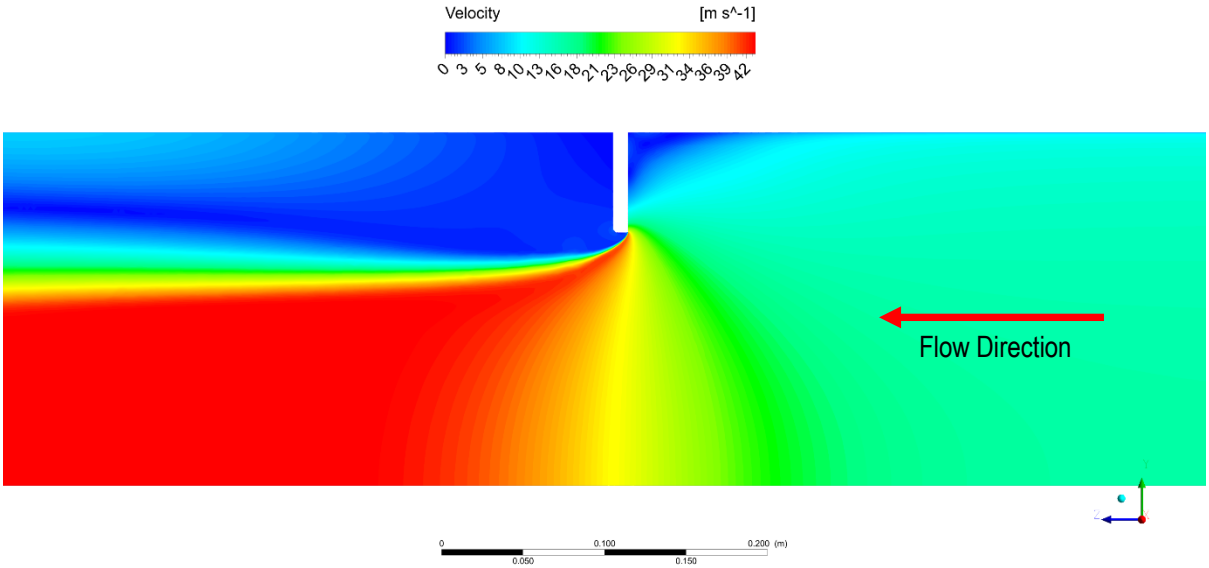

FIGURE 28: VELOCITY CONTOURS FOR CORRECT ORIFICE PLATE INSTALLATION SHOWING ORIFICE PLATE IN DETAIL – PLATE 5036

5.2.2 Reverse Installation

Contours of differential pressure for the case where orifice plate 5036 is installed in the reverse orientation are shown in Figure 29. Velocity contours are also shown in Figure 31 to Figure 33. It can be observed that when the orifice plate is installed in the reverse orientation the velocity profile is different compared to the correct orientation since the separation occurs from the bevel rather than from this sharp edge. This has a significant effect on the pressure drop and therefore contributes to a flow measurement error.

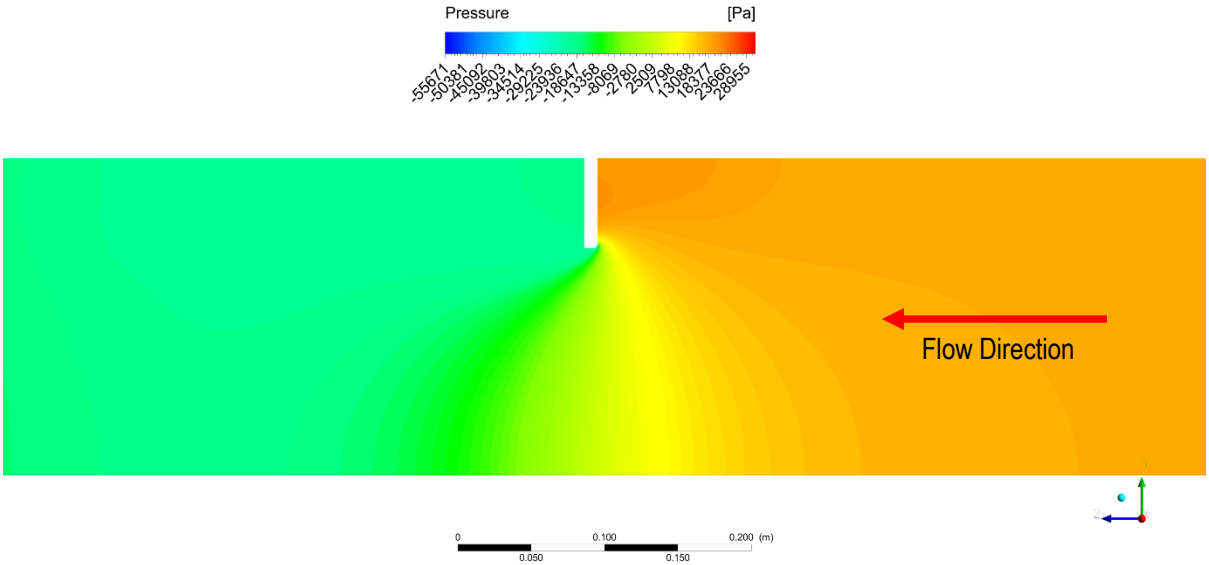

FIGURE 29: DIFFERENTIAL PRESSURE CONTOURS FOR INCORRECT ORIFICE PLATE INSTALLATION– PLATE 5036

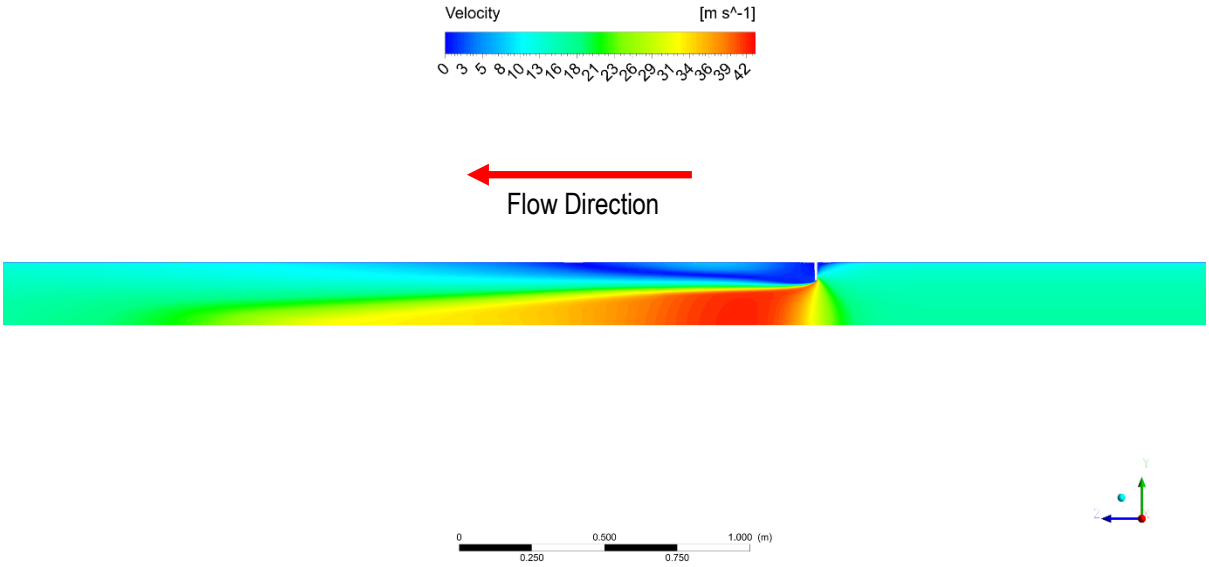

FIGURE 30: VELOCITY CONTOURS FOR INCORRECT ORIFICE PLATE INSTALLATION– PLATE 5036

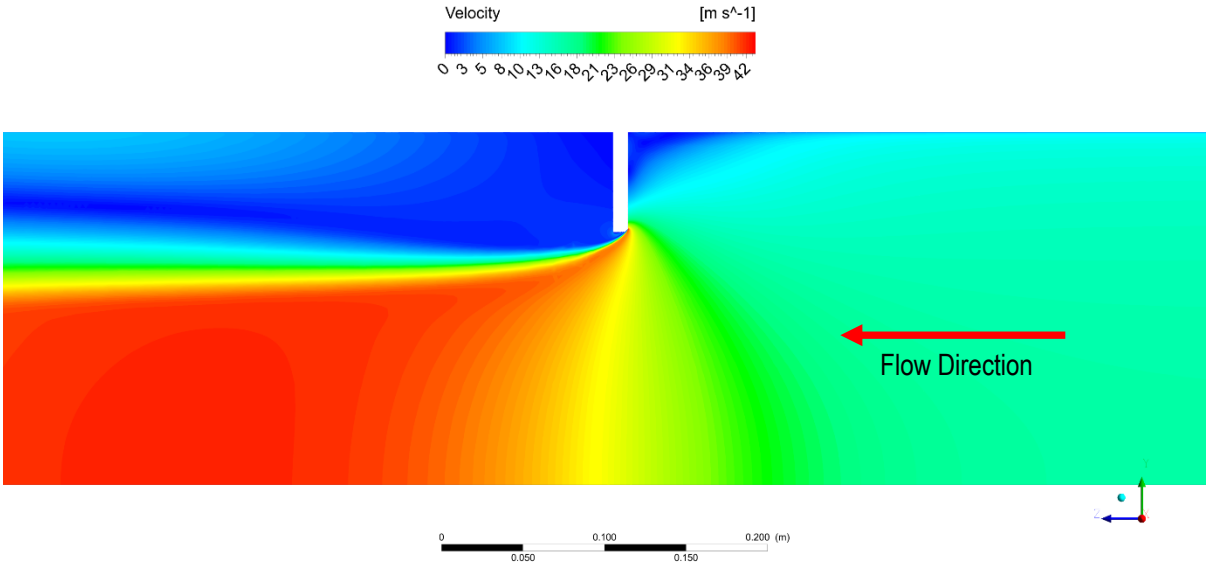

FIGURE 31: VELOCITY CONTOURS FOR INCORRECT ORIFICE PLATE INSTALLATION SHOWING ORIFICE PLATE IN DETAIL – PLATE 295-5

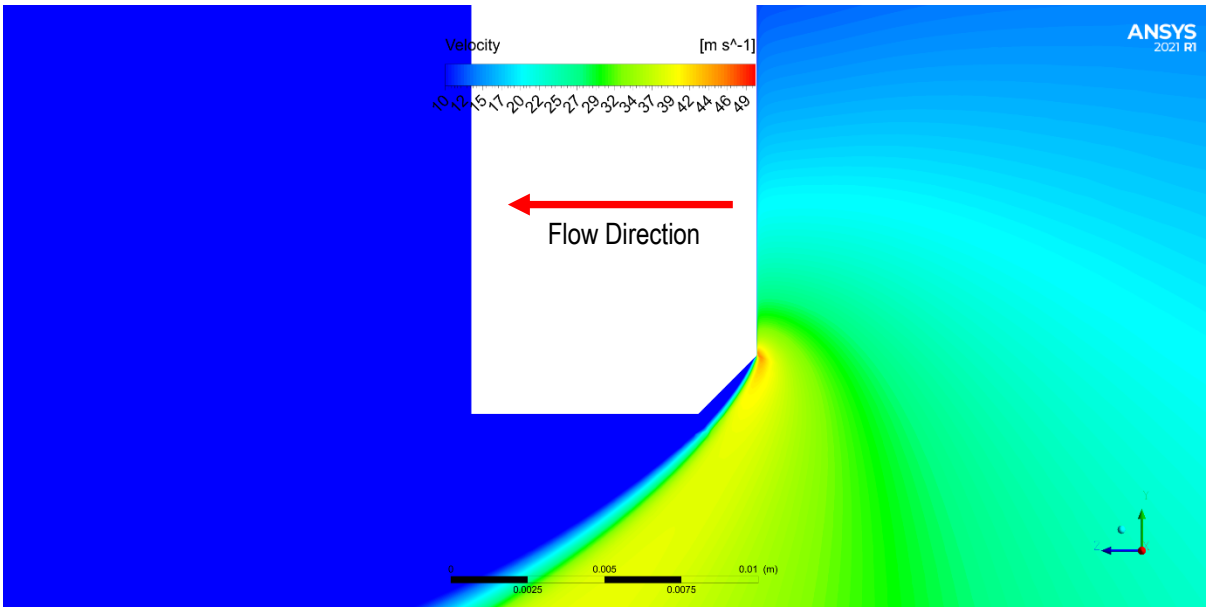

FIGURE 32: VELOCITY CONTOURS FOR INCORRECT ORIFICE PLATE INSTALLATION SHOWING SEPARATION FROM BEVEL

5.2.3 Discharge Coefficients Plate 5036

Table 6 shows the computed discharge coefficient for plate 295-5 installed correctly and the discharge coefficient calculated form the ISO 5167 standard. All of the computed discharge coefficients are within agreement of the ISO 5167 standard which is assessed to be within 1 % values given in the standard.

Table 7 shows the computed ideal discharge coefficient from the CFD analysis, the computed discharge coefficient for the incorrectly installed orifice plate from the CFD simulation and the shift in discharge coefficient due to an incorrect installation. It can be seen that the shift in discharge coefficient is not linear across the range of Reynolds numbers modelled; however, it is significantly closer to linearity than plate 295-5. The meter is still predicted to under read at all points.

TABLE 6: AGREEMENT BETWEEN CFD MODEL OF PLATE 5036 INSTALLED CORRECTLY & ISO 5167

Case	Discharge Coefficient - Standard [1]	Discharge Coefficient - CFD Ideal	CFD Ideal Case Deviation From Standard (%)
Low Flow	0.59768	0.59496	-0.4543
Medium Flow	0.59702	0.59386	-0.52933
Maximum Flow	0.59654	0.59133	-0.87361

TABLE 7: COMPUTED DISCHARGE COEFFICIENTS & FLOW METERING ERROR FOR PLATE 295-5

Case	Discharge Coefficient - CFD Ideal	Discharge Coefficient - CFD Reversed	Shift In Discharge Coefficient (%)
Low Flow	0.59496	0.62663	5.32
Medium Flow	0.59386	0.62559	5.34
Maximum Flow	0.59133	0.62469	5.64

5.2.4 SwRI Validation

A CFD verification exercise was performed in this section based on published test data of reversed orifice plates from SwRI [4]. This was completed to determine how representative the CFD process used here is in capturing the shifts in discharge coefficient due to an orifice plate being reversed.

Four test points were modelled from the report and these are shown below in Table 8:

TABLE 8: TEST POINTS SIMULATED FROM SWRI DATA [4]

Test Point	Orifice Plate Orientation	Reynolds Number
F082600.010	Sharp Edge Facing Upstream	1,632,025
F082600.015	Sharp Edge Facing Upstream	921,857
F082600.030	Bevel Facing Upstream	1,632,983
F082600.035	Bevel Facing Upstream	923,564

Table 9 shows the comparison between the discharge coefficients generated from experiments at SwRI against computed discharge coefficients from CFD. The percentage shift in both cases are within 1 % and therefore in excellent agreement with each other. This is further proof that the CFD approach taken to determine the shift in discharge coefficient for ALREWAS is technically robust.

TABLE 9: COMPARISON OF DISCHARGE COEFFICIENT OBTAINED ROM PHYSICAL TESTING AT SWRI AGAINST DISCHARGE COEFFICIENTS COMPUTED USING CFD

Correctly Installed Point	Incorrectly Installed Point	CFD Discharge Coefficient for Correct Installation	CFD Discharge Coefficient for Reverse Installation	SwRI Shift In Discharge Coefficient (%)	CFD Shift In Discharge Coefficient (%)
F082600.010	F082600.030	0.60969	0.69509	13.78	14.01
F082600.015	F082600.035	0.61108	0.69597	13.69	13.89

6 CONCLUSIONS

NEL have performed Computational Fluid Dynamics to model two orifice plates that were installed incorrectly at the Alrewas facility operated by Cadent.

It was found that in both instances the meter under read across the full range of Reynolds numbers modelled, since when the plate was reversed the actual discharge coefficient was higher.

Orifice plate 295-5 had a maximum shift in discharge coefficient of 7.37 % at the maximum flowrate and plate 5036 had a maximum shift of 5.64 %.

In both cases the computed shift in discharge coefficient was not constant across the range of Reynolds numbers modelled.

In addition to these simulations, further work was undertaken to model experimental work carried out at SwRI to determine how well CFD predicted the shift in discharge coefficients. In both cases analysed the shift in discharge coefficient predicted by CFD was within 1 % of the shift obtained from the experimental work.

7 RECOMMENDATIONS

In this section, general recommendations and observations are highlighted:

1. The diameter ratio for both of the plates is too high and should be reduced because the pressure transducers are ranged from 0 mbar to 1000 mbar although the measured DP rarely exceeds 200 mbar. This is based upon the historical data provided by Cadent which shows very low differential pressures across the orifice plate which only uses the lower end of the pressure transmitters range. A smaller diameter ratio would also reduce the uncertainty in the discharge coefficient.

REFERENCES

1. Measurement of fluid flow by means of pressure differential devices inserted in circular cross-section conduits running full, BS EN ISO 5167-2:2003
2. NEL Quotation 16952 V-05, 28th of April 2021
3. Physical Digital 3D Scanning https://physicaldigital.com/
4. George, D.L, and Morrow, T. B, *Orifice meter operational effects: Orifice meter calibration for backwards-facing orifice plates*, GRI Report Number 01/0074

Information

This report is issued as part of the contract under which the work has been carried out for the client by TUV SUD Limited trading as TÜV SÜD National Engineering Laboratory.

Notes

1. This report may be published in full by the client unless it includes information supplied in confidence by TÜV SÜD National Engineering Laboratory or any third party. Such information, if included within the report, shall be identified as confidential by TÜV SÜD National Engineering Laboratory.
2. The prior written consent of TÜV SÜD National Engineering Laboratory shall be obtained by the client before publication by them of any extract from, or abridgement of, this report.
3. The prior written consent of TÜV SÜD National Engineering Laboratory shall be obtained by the client before publication:
   - Where such publication is made in connection with any public enquiry, legal proceedings or arbitration.
   - Where such publication is made in connection with any company prospectus or similar document.
   - Where the client has notice that TÜV SÜD National Engineering Laboratory is seeking or intends to seek patent or like protection for any intellectual property produced in the course of rendering the services.
4. TÜV SÜD National Engineering Laboratory services are provided subject to terms and conditions acknowledged by our commercial staff and the applicable scope stated in the ISO 9001 certification and/or ISO 17025 accreditation. Services which fall outside the applicable scope of ISO certification and/or accreditation will be stated in this report.

Revision History				
Revision	**Date**	**Description**	**Author(s)**	**Approved By**
1	11/08/21	Initial submission	M. Laing	M. Hanton

Report Production			
Contributor(s)	**Printed Name(s)**	**Signature**	**Date**
Co-author(s)			
Author(s)	Mr Marc Laing		
Reviewer(s)	Dr Sandy Black		
Authorised by	Dr Martin Hanton, Technical Director	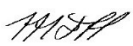	

Report Production			
Contributor(s)	**Printed Name(s)**	**Signature**	**Date**
Customer Revision-Editor			

National Engineering Laboratory

Partner with us today

Point of contact: Marc Laing

Tel: +44 (0) 1355 593889
Email: marc.laing@ tuvsud.com
Web: www.tuvsud.com/en-gb/nel

TUV SUD Limited
Scottish Enterprise Technology Park
East Kilbride
Glasgow, G75 0QF
UK